

High-Throughput Tyrosine Kinase Activity Profiling Identifies FAK as a Candidate Therapeutic Target in Ewing Sarcoma

Brian D. Crompton¹, Anne L. Carlton¹, Aaron R. Thorner¹, Amanda L. Christie³, Jinyan Du⁵, Monica L. Calicchio², Miguel N. Rivera^{4,5}, Mark D. Fleming², Nancy E. Kohl³, Andrew L. Kung⁶, and Kimberly Stegmaier^{1,5}

Abstract

Limited progress has been made in the treatment of advanced-stage pediatric solid tumors despite the accelerated pace of cancer discovery over the last decade. Tyrosine kinase inhibition is one tractable therapeutic modality for treating human malignancy. However, little is known about the kinases critical to the development or maintenance of many pediatric solid tumors such as Ewing sarcoma. Using a fluorescent, bead-based technology to profile activated tyrosine kinases, we identified focal adhesion kinase (FAK, PTK2) as a candidate target in Ewing sarcoma. FAK is a tyrosine kinase critical for cellular adhesion, growth, and survival. As such, it is a compelling target for cancer-based therapy. In this study, we have shown that FAK is highly phosphorylated in primary Ewing sarcoma tumor samples and that downregulation of FAK by short hairpin RNA and treatment with a FAK-selective kinase inhibitor, PF-562271, impaired growth and colony formation in Ewing sarcoma cell lines. Moreover, treatment of Ewing sarcoma cell lines with PF-562271 induced apoptosis and led to downregulation of AKT/mTOR and CAS activity. Finally, we showed that small-molecule inhibition of FAK attenuated Ewing sarcoma tumor growth *in vivo*. With FAK inhibitors currently in early-phase clinical trials for adult malignancies, these findings may bear immediate relevance to patients with Ewing sarcoma. *Cancer Res*; 73(9); 2873–83. ©2013 AACR.

Introduction

Pediatric solid tumors are frequently associated with aberrant activation of transcription factors or loss of tumor suppressor genes. Neither of these oncogenic mechanisms, however, is readily druggable by traditional pharmacologic approaches. Moreover, the sequencing of pediatric cancer genomes is revealing remarkable stability with surprisingly few additional genetic mechanisms of oncogenesis in these diseases (1, 2). Thus, the search for new pediatric cancer therapeutic targets may need to expand beyond next-generation DNA sequencing.

Targeting aberrantly activated tyrosine kinases is one treatment approach that has had recent success in several

types of adult cancers. Selective kinase inhibitor therapy has transformed the care of patients with BCR/ABL-positive chronic myelogenous leukemia (CML; ref. 3), EGF receptor (EGFR)-mutated lung cancer (4), and c-KIT-mutated gastrointestinal stromal tumors (GIST; ref. 5). Over the last year, the B-RAF inhibitor vemurafenib has been approved for patients with B-RAF^{V600E} mutant metastatic or inoperable melanoma, and the ALK inhibitor crizotinib was approved for patients with locally advanced or metastatic ALK-positive non-small cell lung cancer (NSCLC). In pediatric solid tumors, clinical trials testing crizotinib for patients with ALK mutations are ongoing (<http://clinicaltrials.gov/>; NCT00939770). However, few genetically altered kinase targets in pediatric solid tumors have been identified despite emerging data suggesting that activated kinases may play an important role in the development and maintenance of these diseases. For example, in the pediatric solid tumor Ewing sarcoma, insulin-like growth factor-1 receptor (IGF1R) is activated but not mutated, and clinical trials testing IGF1R-targeting antibodies induced clinical responses in a subset of patients with Ewing sarcoma (6, 7). More recently, high levels of spleen tyrosine kinase (SYK) expression were reported as a result of epigenetic deregulation in the pediatric retinal cancer retinoblastoma. SYK targeting with a small-molecule inhibitor induced retinoblastoma cell death *in vitro* and *in vivo* (2).

In this study, we chose to use a screening modality that could rapidly identify highly activated kinases, agnostic to mechanism, and targetable by available drugs. Therefore, we

Authors' Affiliations: ¹Department of Pediatric Oncology, Dana-Farber Cancer Institute, and the Division of Hematology/Oncology, ²Department of Pathology, Children's Hospital Boston; ³Lurie Family Imaging Center, Dana-Farber Cancer Institute; ⁴Department of Pathology, Massachusetts General Hospital, Boston; ⁵Broad Institute of Massachusetts Institute of Technology and Harvard University, Cambridge, Massachusetts; and ⁶Department of Pediatrics, Columbia University Medical Center, New York, New York

Note: Supplementary data for this article are available at Cancer Research Online (<http://cancerres.aacrjournals.org/>).

Corresponding Author: Kimberly Stegmaier, Dana-Farber Cancer Institute, 450 Brookline Ave., D630, Boston, MA 02215. Phone: 617-632-4985; Fax: 617-632-4850; E-mail: kimberly_stegmaier@dfci.harvard.edu

doi: 10.1158/0008-5472.CAN-12-1944

©2013 American Association for Cancer Research.

leveraged a recently described, bead-based tyrosine kinase activity assay that profiles the phosphorylation of a large panel of tyrosine kinases, many of which have available inhibitors (8). We focused on Ewing sarcoma, the second most common bone tumor diagnosed in children, where survival remains poor for patients with metastatic and recurrent disease despite intensive regimens (9, 10). New therapeutic approaches are needed to improve the survival of patients with this disease. Using kinase activity profiling, we evaluated the tyrosine kinase landscape in Ewing sarcoma cell lines and identified focal adhesion kinase (FAK/PTK2) as an actionable, highly activated tyrosine kinase in this disease.

Materials and Methods

Cell culture

A673, EW8, SKNEP, EWS834, and RDES cells were grown in Dulbecco's Modified Eagle's Media (DMEM; Mediatech) with 10% FBS (Sigma-Aldrich). A673 medium was supplemented with 1 mmol/L sodium pyruvate (Invitrogen). TC71 and TC32 were grown in RPMI (Mediatech) with 10% FBS and TTC466, EWS502, and CADO-ES-1 with 15% FBS. Cell lines were provided by Dr. Todd Golub (Broad Institute, Cambridge, MA) except for EWS502 and EWS834, which were a gift from Dr. Jonathan Fletcher (Brigham and Women's Hospital, Boston, MA). All cell lines have unique genotypes and EWS/FLI and EWS/ERG rearrangements were confirmed by RNA sequencing.

Protein extraction and immunoblotting

Whole-cell lysates were extracted in 1× Cell Lysis Buffer (Cell Signaling) supplemented with EDTA-free protease inhibitors and PhosSTOP phosphatase inhibitors (Roche). Western immunoblotting was conducted using standard techniques. Primary antibodies against total FAK, phospho-PYK2 (Y402), total mTOR, phospho-mTOR (S2448), total S6, phospho-S6 (S240/244), total AKT, phospho-AKT (S473), PARP, total ERK, phospho-ERK (T202/Y204), phospho-CAS (Y410), and total SRC were obtained from Cell Signaling. Phospho-FAK (Y397) and total CAS antibodies were from BD Transduction Laboratories, anti-GAPDH from Santa Cruz, anti-vinculin and phospho-SRC (Y416) from Abcam, total PYK2 from Millipore, and anti-actin from Thermo Fisher Scientific.

High-throughput kinase activity profiling

A Luminex immunoassay was conducted on 6 Ewing sarcoma cell lines (EWS502, TC71, TC32, A673, SKNEP, and EW8) and 293FT cells, as previously described (8). Briefly, whole-cell lysates from each cell line were quantified, and equal concentrations of protein were incubated overnight at 4°C with a mixture of 87 validated antibody-coupled Luminex beads (probes) specific for 62 tyrosine kinases. The mixture was then washed and incubated with biotin-labeled 4G10 antibody (Millipore) for 30 minutes at room temperature, washed, and then incubated with 4 µg/mL of SAPE (Molecular Probes) for 10 minutes at room temperature. The conjugates were washed 2 additional times and analyzed on a FlexMAP 3D (Luminex) with xPONENT software (version 4.0; Luminex) to determine the median fluorescent intensity (MFI).

Immunohistochemistry

Fifteen Ewing sarcoma tumor cores were obtained through Institutional Review Board-approved discarded tissue protocols from Massachusetts General Hospital and Children's Hospital Boston. A673 cell lines with and without FAK-directed short hairpin RNA (shRNA) were used for controls. Tumors and controls were examined for phospho-FAK (Y397) protein expression using standard immunohistochemical techniques. A hematoxylin and eosin (H&E)-stained slide was also prepared for each tumor to define the tumor margins. Phospho-FAK expression was scored on a semiquantitative scale based on the percentage of positive staining tumor cells (11).

Lentivirus production and lentiviral transduction

Lentivirus was produced by transfecting HEK-293T cells with the appropriate pLKO.1 lentiviral vector and packaging plasmids (pCMV8.9 and pCMV-VSVG) according to the FuGENE 6 (Roche) protocol. Plasmids were obtained from The RNAi Consortium (Broad Institute). For lentiviral transduction, Ewing sarcoma cells were incubated with 2 mL of virus and 8 µg/mL of polybrene (Sigma-Aldrich) for 2 hours. Cells were selected in puromycin (Sigma-Aldrich) 48 hours posttransduction. shRNA target sequences are listed in Supplementary Table S1.

Small-molecule treatment *in vitro*

Ewing sarcoma cells were plated in 10-cm dishes, allowed to adhere for 24 hours, and then treated with PF-562271 (FAK/PYK2 inhibitor, Haoyuan Chemexpress Co., Ltd.), PD0325901 (MEK inhibitor, Selleck Chemicals), or dasatinib (SRC, BCR/ABL, c-Kit inhibitor, and others, ChemieTek).

Cell viability

ATP content was measured as a surrogate for cell number using the CellTiter-Glo Luminescent Cell Viability Assay (Promega). Luminescence readings were obtained using the FLUOstar Omega microplate reader (BMG Labtech). For experiments with small-molecule treatment, 1.25×10^3 Ewing sarcoma cells were seeded in each well and treated with a range of concentrations. IC₅₀ values were calculated from ATP measurements obtained after 3 days of treatment using log-transformed, normalized data in GraphPad Prism 5.0 (GraphPad Software, Inc.). Cell lines were also treated with compound in 6-cm dishes, trypsinized, and counted by light microscopy using trypan blue exclusion. For experiments using shRNA-transduced cells, 1.25×10^3 cells were seeded per well into 384-well plates on day 3 posttransduction. ATP content was measured on days 3, 6, and 8 posttransduction.

Colony formation in methylcellulose matrix

Approximately 3.75×10^3 cells were dissolved into 1.5 mL of methylcellulose matrix (ClonaCell-TCS Medium, Stemcell Technologies), plated into gridded 6-cm plates (Thermo Fisher Scientific), and incubated for at least 10 days. Colonies from 100 squares were counted using a Nikon inverted microscope.

Flow cytometry

Cells undergoing apoptosis were identified by flow cytometry (FACSCalibur, BD Biosciences) using the ApoAlert Annexin V-FITC Apoptosis Kit (Clontech). For intracellular phosphoprotein staining, cells were fixed and permeabilized using the BD Cytofix/Cytoperm Kit (BD Biosciences) and stained with phycoerythrin (PE) anti-phospho-S6 (S240, BD Biosciences) and analyzed by flow cytometry (BD FACSCanto II).

In vivo studies

Approximately 1×10^6 A673 cells transduced with either a control or 2 different FAK-directed shRNAs were suspended in 30% Matrigel and subcutaneously injected into the flank of 6-week-old female NCr nude mice ($n = 8$ per condition). Tumor volume was measured periodically using calipers to monitor tumor growth (volume = $0.5 \times \text{length} \times \text{width}^2$).

Approximately 4.2×10^6 A673 cells were mixed with 30% Matrigel and injected subcutaneously into 8-week-old female NCr nude mice. When the average tumor volume in all animals reached approximately 100 mm^3 , twice-daily treatment was administered by oral gavage with 200 mg/kg PF-562271 (in a volume of 10 ml/kg) or vehicle control (0.5% hydroxypropyl methylcellulose and 0.2% Tween 80 in sterile water; $n = 6$ per condition). Ten-week-old male NSG mice were used for *in vivo* experiments with TC32 cells to improve tumor engraftment with this cell line. In this model, several mice experienced toxicity when treated with PF-562271 at 200 mg/kg twice daily (data not shown). Therefore, after injection of approximately 5×10^6 TC32 cells in 30% Matrigel, animals began treatment with PF-562271 at 100 mg/kg or vehicle control ($n = 8$ per condition) every 12 hours when tumor volumes reached 100 mm^3 . This dose was well tolerated, and at day 13, the dose was escalated to 150 mg/kg. Tumor volumes were measured with calipers. Animals were sacrificed when tumor volumes exceeded 2,000 mm^3 .

Statistical methods

The Student *t* test or 1- or 2-way ANOVA with Tukey *post hoc* tests were used to compare groups. Statistical analyses were conducted using GraphPad Prism 5.0 or SigmaStat 3.5 (Aspire Software International).

Results

FAK is active in Ewing sarcoma

We profiled the activity of 62 unique tyrosine kinases in 6 Ewing sarcoma cell lines using a Luminex bead-based assay (Fig. 1A; ref. 8). The majority of kinases profiled displayed low phosphorylation levels in Ewing sarcoma cell lines, which was similar to the phosphorylation levels observed in the 293FT cell line control. However, SRC kinase (SRC), extracellular signal-regulated kinases (ERK), and FAK were highly phosphorylated in the panel of Ewing sarcoma cell lines (Fig. 1B; Supplementary Table S2) relative to the control. Treatment of Ewing sarcoma cell lines with the SRC inhibitor dasatinib and the MEK inhibitor PD0325901 had minimal effect on cell viability at concentrations that inhibited phosphorylation of SRC and ERK, respectively (Supplementary Fig. S1). Therefore, we focused our efforts

on evaluating the importance of FAK activity in Ewing sarcoma.

First, we show that FAK is highly phosphorylated across a panel of 10 Ewing sarcoma cell lines, including those screened in the profiling assay, by Western immunoblotting (Fig. 1C). Because FAK is known to play a role in adhesion, it was important to confirm that FAK activity was not merely a phenomenon of cell lines growing in culture (12). Therefore, we conducted immunohistochemical (IHC) staining for phosphorylated FAK (Y397) in 15 primary Ewing sarcoma tumor samples using Ewing sarcoma cell lines with or without FAK-directed shRNA as controls (Fig. 1D and Table 1). All but one tumor specimen stained positive for the presence of phosphorylated FAK, showing that FAK is expressed and activated in the majority of Ewing sarcoma tumors.

FAK suppression impairs Ewing sarcoma cell growth and colony formation

To test the dependency of Ewing sarcoma on the presence of activated FAK for cell growth and colony formation, we infected cell lines with lentivirus containing shRNA constructs targeting multiple different regions of the FAK transcript. We identified 5 unique shRNA sequences that robustly downregulated FAK protein levels (Supplementary Fig. S2 and Supplementary Table S1) and chose 2 shRNAs that gave consistent knockdown across our panel of cell lines (Fig. 2A) for further study. The downregulation of FAK through shRNA transduction resulted in significantly impaired cell growth (using ATP content as a surrogate for cell number) across a panel of 4 cell lines (Fig. 2B), including one line with an EWS/ERG rearrangement (TTC466). FAK downregulation also inhibited Ewing sarcoma cell line colony formation in a methylcellulose matrix, showing that FAK activity contributes to anchorage-independent growth in Ewing sarcoma cell lines (Fig. 2C).

A common therapeutic modality for inhibiting kinases is to use small-molecule inhibitors. These compounds, however, do not downregulate total protein as is the case for shRNAs, but rather they inhibit kinase activity. Therefore, it was important to determine whether the inactivation of FAK activity was sufficient to induce the effects observed after shRNA-induced downregulation of FAK. We thus tested the effects of PF-562271, a selective inhibitor of both FAK and proline-rich tyrosine kinase 2 (PYK2), a FAK-related family member, on cell growth and colony formation in Ewing sarcoma cell lines (13). Seven cell lines were treated for 5 days with PF-562271 across a range of concentrations using 2-fold serial dilutions. Treatment with PF-562271 impaired cell viability in all cell lines, with an average IC₅₀ of 2.4 $\mu\text{mol/L}$ after 3 days of treatment (Fig. 3A). TC32 and A673 were the 2 most sensitive cell lines, with IC₅₀ concentrations of 2.1 and 1.7 $\mu\text{mol/L}$, respectively. After confirming that this luminescent ATP detection assay is a faithful surrogate for cell number in Ewing sarcoma cell lines (Supplementary Fig. S3), we evaluated the effects of PF-562271 in a time course. FAK inhibition impaired Ewing sarcoma cell growth in all cell lines tested (Supplementary Fig. S4). We then tested four Ewing sarcoma cell lines for their ability to form colonies in a methylcellulose matrix after

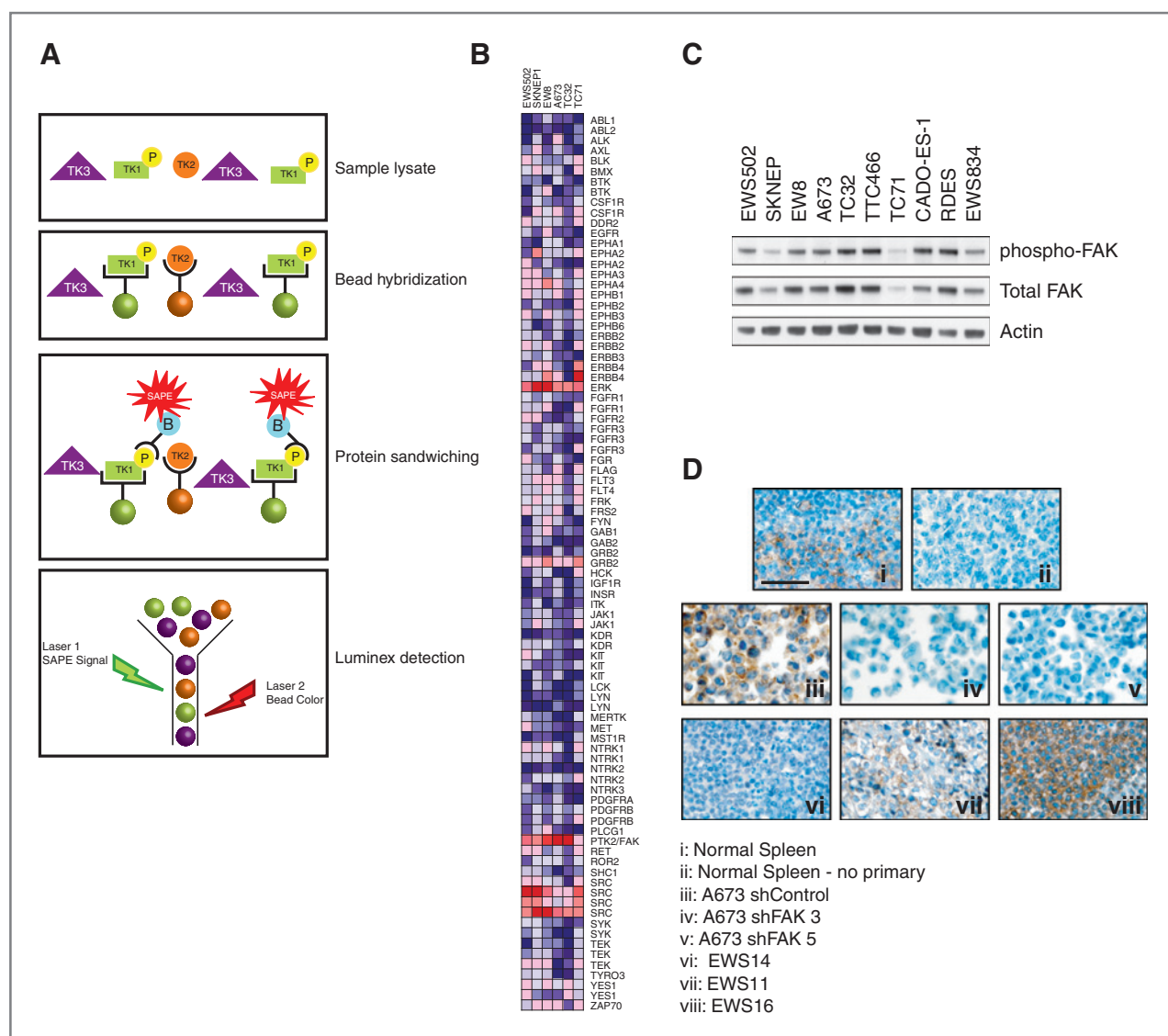


Figure 1. FAK is activated in Ewing sarcoma. **A**, schematic representation of the Luminex-based kinase profiling assay used to identify FAK (also known as PTK2) as a highly phosphorylated protein tyrosine kinase in Ewing sarcoma. **B**, heatmap illustrating tyrosine kinase phosphorylation across 6 Ewing sarcoma cell lines. Median fluorescent intensity values for each kinase-specific probe in the Ewing sarcoma cell lines were divided by the respective median fluorescent intensity values for the 293FT control. Relative values were then normalized across each cell line on a scale of -3 to 3 and displayed as a heatmap using GenePattern software (version 3.3.3; Broad Institute). SRC, ERK, and FAK are highly phosphorylated in the panel of cell lines tested. **C**, Western immunoblot showing total FAK and phospho-FAK expression levels across a panel of 10 Ewing sarcoma cell lines using actin as the loading control. **D**, IHC staining for phospho-FAK in normal spleen with and without phospho-FAK primary antibody (i and ii), A673 cells with and without FAK downregulation by shRNA (iii–v), and Ewing sarcoma primary tumor cores (vi–viii). Scale bar, 1 mm.

24 hours of PF-562271 treatment across a range of concentrations. Cells were continuously exposed to PF-562271 in the methylcellulose matrix. Colony formation was significantly reduced with PF-562271 treatment in a concentration-dependent manner and corresponding to the IC₅₀ of each line (Fig. 3B).

Inhibition of FAK induces apoptosis in Ewing sarcoma cell lines

In some cell lines treated with PF-562271, we noted a decrement in cell number over time (Supplementary Fig.

S4), indicating that FAK inhibition may also induce apoptosis in Ewing sarcoma. To test this hypothesis, we treated 4 Ewing sarcoma cell lines with PF-562271 and measured apoptosis using Annexin V/propidium iodide staining. Apoptosis was significantly increased in a time- and concentration-dependent manner across all lines tested (Fig. 3C). To confirm this finding, we measured PARP cleavage by Western immunoblotting in Ewing sarcoma cells treated with PF-562271 for 24 hours. There was a concentration-dependent increase in PARP cleavage, which correlated with our flow cytometric findings (Fig. 3D).

Table 1. Phospho-FAK IHC staining intensity in A673 controls and Ewing sarcoma primary tumor cores

Sample ID	Score 0–2
A673 shControl	1+
A673 shFAK 3	Occasional single cell
A673 shFAK 5	Occasional single cell
EWS1	1+
EWS2	0–1+
EWS3	2+
EWS4	1+
EWS5	1+
EWS6	0–1+
EWS7	1–2+
EWS8	1+
EWS10	1+
EWS11	1+
EWS12	1+
EWS13	1+
EWS14	0
EWS15	0–1+
EWS16	2+

FAK inhibition downregulates mTOR and CAS

The mTOR pathway is reported to be activated in a subset of Ewing sarcoma tumors and is a likely oncogenic driver (14–16). FAK is a known upstream regulator of AKT in normal tissue and models of cancer, suggesting a possible mechanistic link in Ewing sarcoma (17, 18). Therefore, we examined the effects of FAK inhibition on the AKT/mTOR pathway. First, Ewing sarcoma cells were serum-starved overnight to prevent oversaturation of this pathway by serum growth factor stimulation. Then, cells were treated with multiple concentrations of PF-562271 for 6 hours, followed by stimulation with IGF-1 for 2 hours. Treatment with PF-562271 downregulated AKT (S473), mTOR (S2448), and S6 (S240/244) phosphorylation at concentrations that impair cell growth and colony formation (Fig. 4A and Supplementary Table S3). We next confirmed that S6 phosphorylation was downregulated in cell lines treated with PF-562271 in a dose response by intracellular phospho-specific flow cytometry (Fig. 4B).

FAK is also reported to regulate the activity of Crkl-associated substrate (CAS) and the MEK/ERK pathway in some cellular contexts (12, 19, 20). Therefore, we examined the effects of FAK inhibition on CAS and ERK activity in A673 and TC32 cell lines after treatment with PF-562271. We found that FAK inhibition resulted in downregulation of CAS phosphorylation but not ERK (Fig. 4C). We then identified 3 unique CAS-directed shRNAs targeting different regions of the CAS transcript that robustly downregulate CAS expression (Fig. 4D and Supplementary Table S1). CAS downregulation in A673 cells had only a modest effect on cell growth and a variable effect on colony formation (Fig. 4E), suggesting that CAS inhibition alone cannot account for the effects observed with FAK inhibition in Ewing sarcoma.

FAK contributes to tumor establishment and growth in xenograft models of Ewing sarcoma

To confirm that loss of FAK impairs tumor initiation *in vivo*, FAK levels were downregulated via shRNA in A673 cells and injected subcutaneously in NCr nude mice. Because FAK suppression is selected against over time, we limited the study to 3 weeks. FAK downregulation significantly impaired tumor establishment and growth in this xenograft model of Ewing sarcoma (Fig. 5A).

We also tested whether the inhibition of FAK activity by treatment with PF-562271 could inhibit progression in established tumors using 2 xenograft models of Ewing sarcoma. NCr nude and NSG mice were subcutaneously injected with A673 and TC32 cells, respectively, and allowed to develop measurable tumors. The animals were then treated with either vehicle or PF-562271 until the animals were sacrificed. Treatment with PF-562271 significantly inhibited tumor growth compared with the controls showing that FAK activity contributes to tumor growth in Ewing sarcoma (Fig. 5B and C).

Discussion

Ewing sarcoma is a rare pediatric cancer with an incidence of approximately one case per million people in the United States (21). Although progress has been made in treating this disease with conventional chemotherapy combined with surgery or radiation for local control, outcomes for relapsed and metastatic disease are notably poor (9, 10, 22). Furthermore, an emerging literature on the long-term side effects of these conventional treatment modalities in pediatric cancer survivors leaves us unsatisfied with the current standard of care (23). However, for many rare pediatric cancers, the tumor driver events are too often the expression of an aberrant transcription factor, such as the EWS/FLI rearrangement in Ewing sarcoma (24), or loss of a tumor suppressor gene, both challenging to target using conventional drug screening approaches. Therefore, it is critical to prioritize efforts to identify more tractable targets in these rare, but devastating, childhood diseases.

Here, we took an alternative approach to identify new, potentially more tractable therapeutic targets in Ewing sarcoma. In light of the recent successes targeting kinases in the treatment of patients with cancer, we focused on this drugable target space. We profiled a panel of tyrosine kinases, inclusive of the majority of kinases with available inhibitors, in a collection of Ewing sarcoma cell lines. Because virtually all tyrosine kinases are phosphorylated when activated, tyrosine kinase phosphorylation was used as a proxy for kinase activity in this assay. One strength of this approach is that kinase activation will be identified independent of the mechanism of activation. While many cancer-promoting kinase activation events involve copy number gain or DNA mutation/rearrangement, there are recent examples of kinase activation via nongenetic events. For example, SYK was reported to be overexpressed in retinoblastoma via epigenetic regulation (2) and the tyrosine kinase Met (MET) is activated in many cancers by overexpression of the ligand, hepatocyte growth factor (HGF; ref. 25).

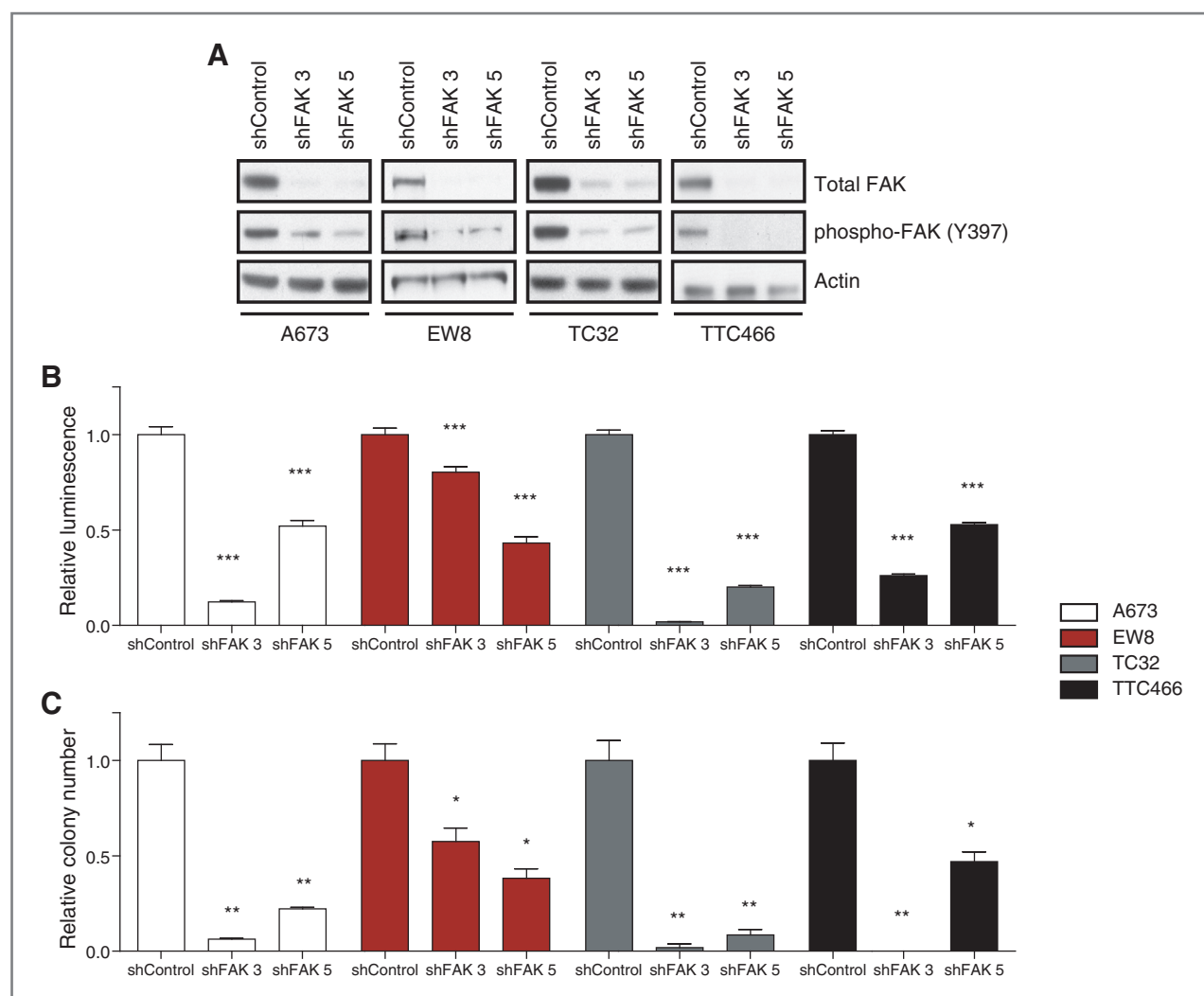


Figure 2. Suppression of FAK protein levels impairs cell growth and colony formation. **A**, Western immunoblots showing downregulation of FAK levels by transduction with FAK-directed shRNAs. **B**, effects of genetic downregulation of FAK on cell growth measured by a luminescent ATP detection assay. Relative luminescence was calculated by dividing each day 8 luminescence value by the average day 3 value. Each value was then divided by the average value of the shControl-treated cells. **C**, colony formation in methylcellulose relative to a control shRNA. Shown are the mean (14–16 replicates for viability and 2–4 for colony formation) \pm SEM. *, P < 0.05; **, P < 0.01; ***, P < 0.001 by 1-way ANOVA with Tukey post hoc test.

SRC kinase, ERK, and FAK were highly phosphorylated in this screen. While SRC kinase and ERK pose attractive targets, chemical inhibition at concentrations eliminating phosphorylation had minimal effect on cell viability in the Ewing sarcoma cell lines evaluated. Therefore, our study focused on the validation of FAK as a potential therapeutic target in Ewing sarcoma. FAK is a non-receptor tyrosine kinase and central regulator of integrin signaling that mediates many normal cellular functions including adhesion, migration, survival, growth, and differentiation. FAK activation is initiated through a variety of extracellular signals that allow the cell to adapt to changes in the surrounding environment (26, 27). Activation of FAK leads to autophosphorylation at Y397, triggering an association with the SH2 domain of many signaling proteins including SRC, phosphoinositide 3-kinase (PI3K), phospholipase C, gamma 1 (PLCG1), and growth factor receptor-bound

protein 7 (GRB7; refs. 28–31). Aberrant upregulation of FAK activity is a frequent event in cancer, promoting cell growth, survival, and invasion (32–34), and FAK activation is also associated with poor outcomes and increased metastatic potential (35). Downregulation of FAK activity in numerous cancer models impairs survival *in vitro* and inhibits tumor growth in xenograft models (13, 33).

Previous studies in Ewing sarcoma have alluded to a potential role for adhesion molecules in the pathogenesis of this disease. A gene expression-based study identified panels of highly expressed genes associated with poor prognosis in Ewing sarcoma. Among the gene sets identified was a collection of genes regulating cell adhesion, supporting a role for adhesion molecules in Ewing sarcoma (36). In a second study, FAK transcript levels were found to be elevated in a panel of Ewing sarcoma family cell lines compared with normal

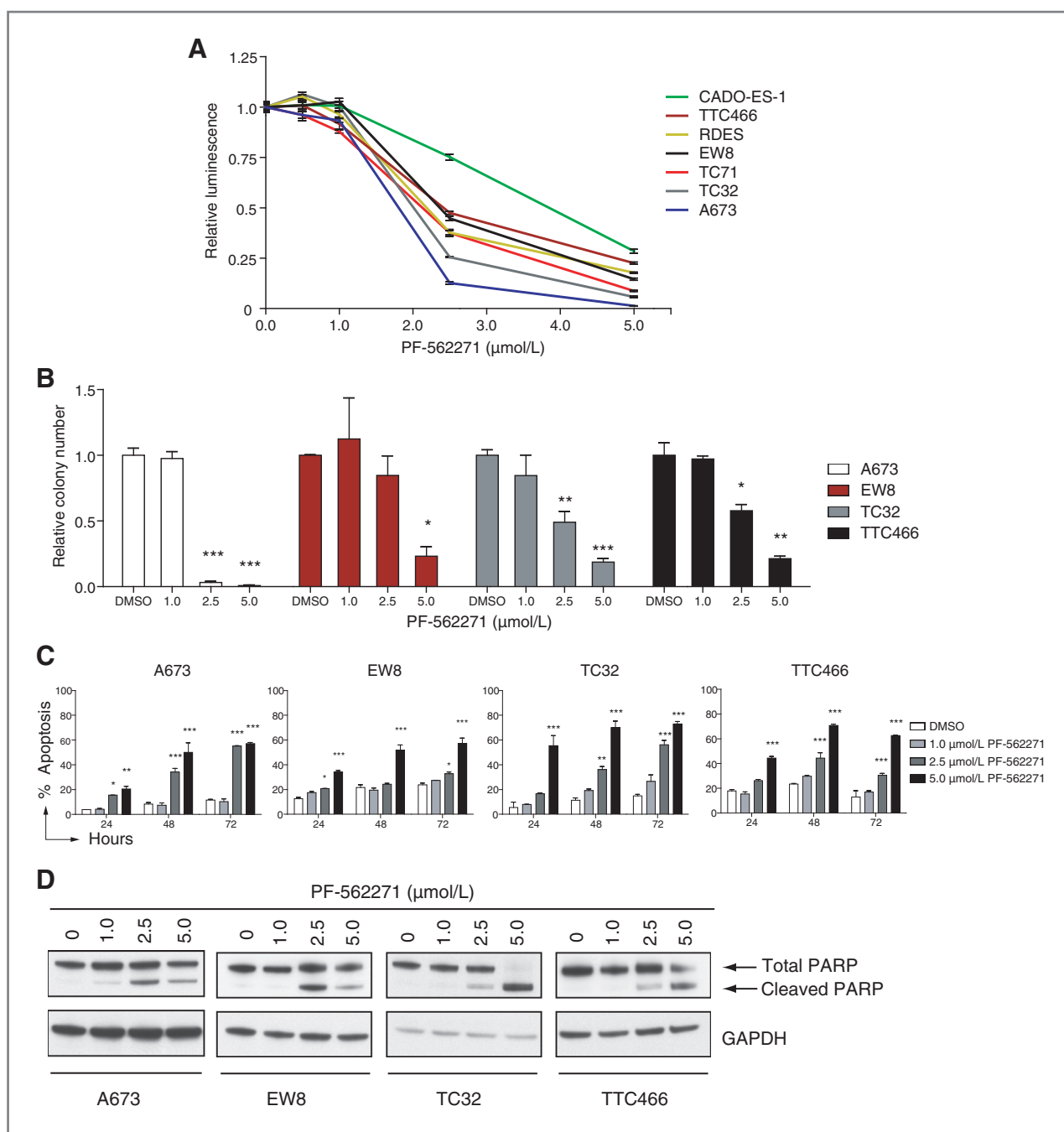


Figure 3. Small-molecule inhibition of FAK impairs cell viability and colony formation and induces apoptosis. **A**, effects of three days of treatment with PF-562271 on Ewing sarcoma cell lines (average $IC_{50} = 2.4 \mu\text{mol/L}$). Relative luminescence was calculated by dividing each luminescence value by the average dimethyl sulfoxide (DMSO) value. Shown are the mean of 8 replicates \pm the SEM. **B**, effects of PF-562271 treatment on colony formation in Ewing sarcoma cell lines relative to DMSO (1-way ANOVA, Tukey post hoc test; *, $P < 0.05$; **, $P < 0.01$; ***, $P < 0.001$). Mean relative colony number (\pm SEM) of 4 replicates is shown. **C**, effects of PF-562271 treatment on apoptosis in a time- and concentration-dependent manner in Ewing sarcoma cell lines (2-way ANOVA, Tukey post hoc test; *, $P < 0.05$; **, $P < 0.01$; ***, $P < 0.001$). Shown are the mean percent of cells undergoing apoptosis (\pm SEM) of 2 replicates. **D**, Western immunoblots depict the protein levels of total PARP and cleaved PARP following 24-hour treatment with PF-562271. Glyceraldehyde-3-phosphate dehydrogenase (GAPDH) was included as the loading control.

fibroblasts (37). Another study found that endoglin expression in Ewing sarcoma tumors is associated with increased expression of several proteins, including FAK, and is associated with poor outcome (38). Recently, a phosphoproteomics screen

identified FAK phosphorylation in sarcoma cell lines including an Ewing sarcoma cell line (39).

The *FAK*(*PTK2*) gene is located on chromosome 8. *FAK* gene amplification has been reported in several malignancies and

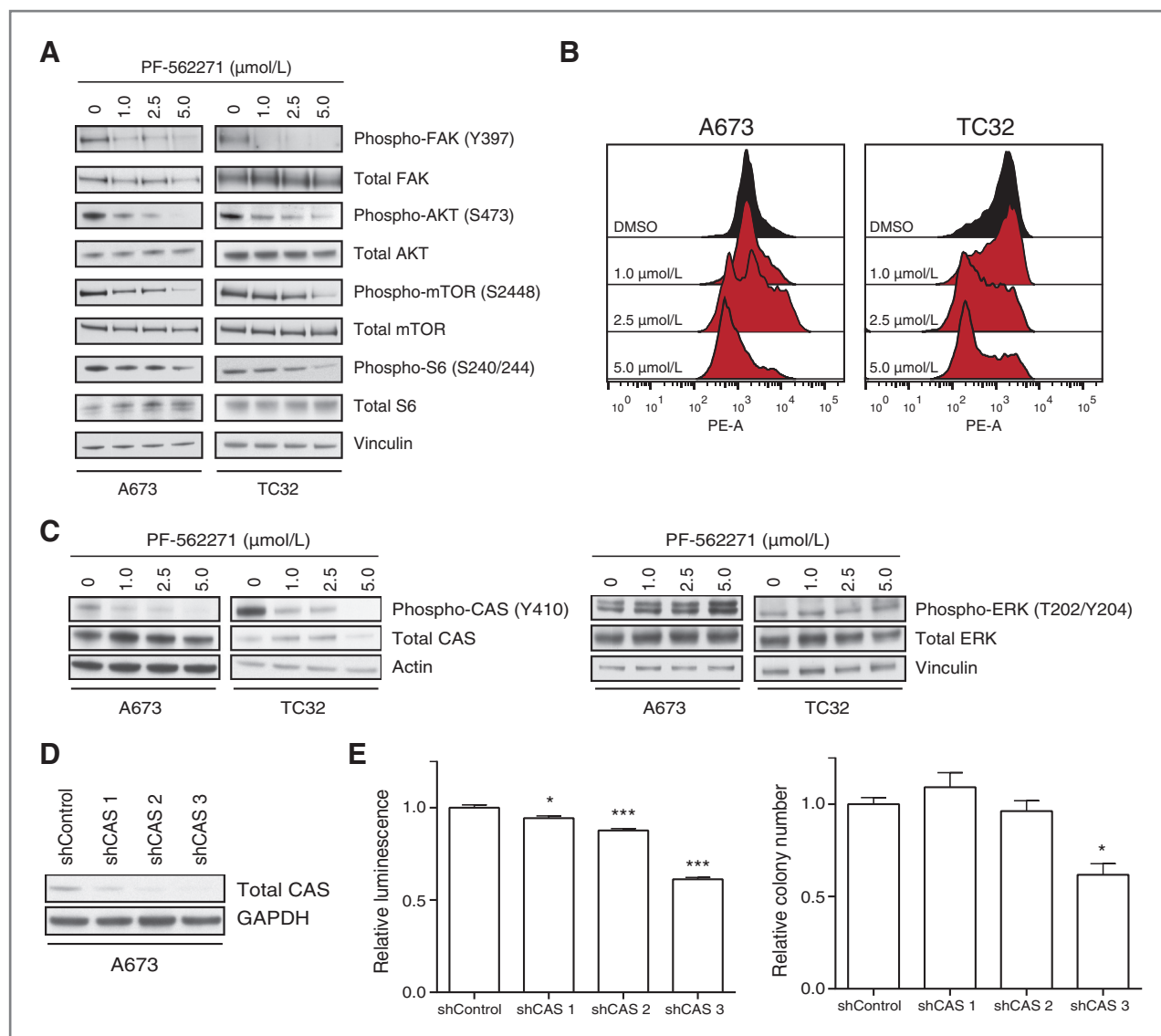


Figure 4. FAK inhibition downregulates the AKT/mTOR pathway and CAS activity. **A**, protein levels measured by Western immunoblotting for AKT/mTOR pathway proteins in A673 and TC32 cells serum-starved overnight, treated with PF-562271 for 6 hours, and then stimulated with IGF-1 for 2 hours. Vinculin was used as the loading control. **B**, histograms of intracellular phospho-S6 (S240) levels in live cells stained with anti-phospho-S6 and measured by flow cytometry in A673 and TC32 cells treated overnight with PF-562271. **C**, Western immunoblots showing downregulation of CAS by 3 unique shRNA constructs but not phospho-ERK in A673 and TC32 cells after treatment with PF-562271. **D**, downregulation of CAS by 3 unique shRNA constructs has a modest effect on (E) cell growth and colony formation in methylcellulose relative to a control shRNA (1-way ANOVA, Tukey post hoc test; *, $P < 0.05$; **, $P < 0.01$; ***, $P < 0.001$). Relative luminescence was calculated by dividing each day 6 luminescence value by the average day 3 value. Each value was then divided by the average value of the shControl-treated cells. Relative luminescence and relative colony number are shown as the mean of 14 replicates and 2 replicates, respectively (\pm SEM).

has variable association with increased expression of FAK protein (40, 41). Interestingly, in Ewing sarcoma, chromosome 8 copy number gain is a frequent genetic event, potentially implicating FAK in the pathogenesis of this disease (42). However, despite reports of FAK expression in Ewing sarcoma cell lines, to our knowledge, this is the first study to show that FAK is highly phosphorylated in both Ewing sarcoma cell lines and Ewing sarcoma primary tumor samples, and it is the first to describe the dependency of Ewing sarcoma on FAK activity. Our *in vitro* and *in vivo*

studies using both FAK-directed shRNA and chemical inhibition of FAK, show that Ewing sarcoma is dependent on FAK activity for growth, colony formation, tumor establishment, and tumor progression.

Efforts to develop targeted therapy for Ewing sarcoma are still in their infancy. However, studies have shown that downregulation of the AKT/mTOR pathway has antitumor activity, and inhibiting this pathway may be a reasonable approach to targeting this disease (14, 15). In fact, there has been modest success in treating relapsed and refractory Ewing sarcoma

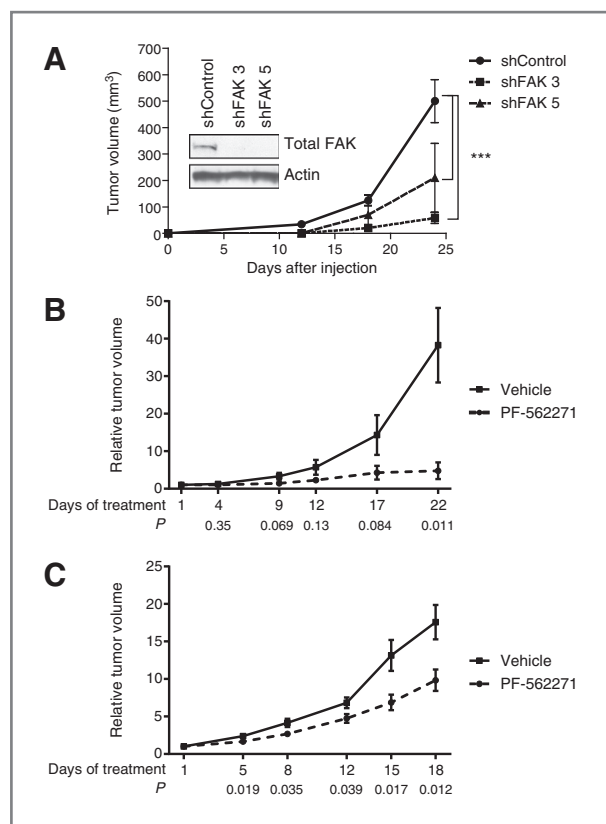


Figure 5. FAK inhibition impairs tumor engraftment and tumor progression *in vivo*. **A**, average size (mean \pm SEM) of subcutaneous tumors in NCr mice. Tumors were grown from subcutaneous injection of A673 cells transduced with control or FAK-directed shRNA. Tumor volume was measured periodically until sacrifice 24 days postinjection. Western immunoblotting displays the total FAK levels from the control and knockdown lines in cells before injection. Tumor volume was significantly reduced 24 days postinjection (two-way repeated measures ANOVA; ***, $P < 0.001$). **B** and **C**, PF-562271 treatment significantly reduced tumor growth after subcutaneous injection of A673 and TC32 cells, respectively, in human tumor xenograft models of Ewing sarcoma. Relative tumor volumes were calculated by dividing the tumor volume measurement for each animal by the corresponding day 0 measurement for that animal. P values were calculated by the Student *t* test for each time point. Shown are the mean relative tumor volumes \pm SEM.

tumors with IGF1R-targeted antibody therapy (7). Studies have shown that the inhibition of IGF1R leads to downregulation of AKT and mTOR in Ewing sarcoma (43). Furthermore, there is an emerging literature that champions the targeting of multiple nodes in a critical cancer pathway by using a combination of inhibitors to improve response and prevent the development of resistance (44). An RNAi screen in Ewing sarcoma determined that downregulation of the mTOR pathway sensitized Ewing sarcoma cells to IGF1R inhibition, and a recent phase I study showed tumor responses in a subset of patients with refractory Ewing sarcoma using IGF1R- and mTOR-targeted combination therapy (45, 46). While FAK activation may have multiple cancer-promoting effects in Ewing sarcoma, treatment of Ewing sarcoma cells with PF-562271 downregulated the activity of the AKT/mTOR pathway, suggesting that the inhibition of FAK is not only an attractive approach to treating

Ewing sarcoma but also may offer a logical candidate for combination therapy with IGF1R- or AKT/mTOR-targeted treatment. Because PF-562271 is also reported to inhibit PYK2 (13), which is variably expressed in Ewing sarcoma cell lines (Supplementary Fig. S5), another possibility is that, in a subset of Ewing sarcoma cell lines, PYK2 inhibition contributes to the downregulation of the AKT/mTOR pathway.

In exploring other reported downstream effectors of FAK, we also found that treatment with PF-562271 in Ewing sarcoma cells inhibited CAS. Genetic downregulation of CAS, however, had only a modest effect on cell growth and colony formation in Ewing sarcoma cells, suggesting that CAS inhibition alone is not sufficient to explain the effects of FAK inhibition *in vitro*. CAS has been shown to play a role in cancer cell invasion and migration (47). One study reported that in a glioblastoma cell line ectopically expressing PTEN, overexpression of CAS restored invasion and migration but did not fully rescue cell growth (48). Because of the reported role of FAK/CAS in cancer metastasis, it will be important to determine in future studies whether this axis is relevant to the metastasis of Ewing sarcoma tumors. Moreover, additional pathways downstream of FAK, not explored in the current study, may be contributing to the anti-Ewing sarcoma phenotype seen with FAK inhibition.

Finally, it is important to note that there are several recently completed or ongoing early-phase clinical trials using FAK inhibitors to treat adult patients with solid tumors (<http://clinicaltrials.gov/>; NCT00666926, NCT00996671, NCT00787033, NCT01138033). Early reports for one of these inhibitors suggest that these drugs are well tolerated. Interestingly, several patients had disease response by positron emission tomography (PET) and prolonged stabilization of disease while on treatment (49). While it is still too early to draw conclusions from these clinical trials, the availability of clinically relevant FAK inhibitors, combined with the results described in our study, suggest the potential for rapid translation to the clinic for patients with Ewing sarcoma.

Disclosure of Potential Conflicts of Interest

No potential conflicts of interest were disclosed.

Authors' Contributions

Conception and design: B.D. Crompton, N.E. Kohl, K. Stegmaier
Development of methodology: B.D. Crompton, J. Du, M.D. Fleming, A.L. Kung, K. Stegmaier
Acquisition of data (provided animals, acquired and managed patients, provided facilities, etc.): A.L. Carlton, A.R. Thorner, A.L. Christie, J. Du, M.L. Calicchio, M.N. Rivera, M.D. Fleming, N.E. Kohl, K. Stegmaier
Analysis and interpretation of data (e.g., statistical analysis, biostatistics, computational analysis): B.D. Crompton, A.L. Carlton, J. Du, M.L. Calicchio, M.D. Fleming, N.E. Kohl, A.L. Kung, K. Stegmaier
Writing, review, and/or revision of the manuscript: B.D. Crompton, A.R. Thorner, M.L. Calicchio, M.D. Fleming, A.L. Kung, K. Stegmaier
Administrative, technical, or material support (i.e., reporting or organizing data, constructing databases): B.D. Crompton, A.L. Carlton, A.L. Christie, M.L. Calicchio, M.D. Fleming
Study supervision: B.D. Crompton, M.D. Fleming, N.E. Kohl, A.L. Kung, K. Stegmaier

Acknowledgments

The authors thank Sara Akhavanfarid for the preparation of primary tumor samples; Kristen Jones, Tanya Tupper, and Amy Saur for their assistance with the xenograft studies; and Swapnil Mehta, Mounica Vallurupalli, and Linda Ross for their technical contributions.

Grant Support

This work was supported by Cookies for Kids' Cancer, Golf Fights Cancer, Brian MacIsaac Sarcoma Foundation (K. Stegmaier); Hyundai Hope on Wheels, Bear Necessities Pediatric Cancer Foundation, Pedal for Pediatrics (B.D. Crompton); Aid for Cancer Research (A.R. Thorner); Burroughs Wellcome Fund (M.N. Rivera); and the Howard Hughes Medical Institute (K. Stegmaier and M.N. Rivera). K. Stegmaier is also supported by a Stand-Up-to-Cancer Innovative Research Grant,

a program of the Entertainment Industry Foundation (SU2C-AACR-IRG0509).

The costs of publication of this article were defrayed in part by the payment of page charges. This article must therefore be hereby marked *advertisement* in accordance with 18 U.S.C. Section 1734 solely to indicate this fact.

Received May 21, 2012; revised January 24, 2013; accepted February 7, 2013; published OnlineFirst March 27, 2013.

References

- Lee RS, Stewart C, Carter SL, Ambrogio L, Cibulskis K, Sougnez C, et al. A remarkably simple genome underlies highly malignant pediatric rhabdoid cancers. *J Clin Invest* 2012;122:2983–8.
- Zhang J, Benavente CA, McEvoy J, Flores-Otero J, Ding L, Chen X, et al. A novel retinoblastoma therapy from genomic and epigenetic analyses. *Nature* 2012;481:329–34.
- O'Brien SG, Guilhot F, Larson RA, Gathmann I, Baccarani M, Cervantes F, et al. Imatinib compared with interferon and low-dose cytarabine for newly diagnosed chronic-phase chronic myeloid leukemia. *N Engl J Med* 2003;348:994–1004.
- Paez JG, Janne PA, Lee JC, Tracy S, Greulich H, Gabriel S, et al. EGFR mutations in lung cancer: correlation with clinical response to gefitinib therapy. *Science* 2004;304:1497–500.
- Demetri GD, von Mehren M, Blanke CD, Van den Abbeele AD, Eisenberg B, Roberts PJ, et al. Efficacy and safety of imatinib mesylate in advanced gastrointestinal stromal tumors. *N Engl J Med* 2002;347:472–80.
- Scotlandi K, Benini S, Sarti M, Serra M, Lollini PL, Maurici D, et al. Insulin-like growth factor I receptor-mediated circuit in Ewing's sarcoma/peripheral neuroectodermal tumor: a possible therapeutic target. *Cancer Res* 1996;56:4570–4.
- Pappo AS, Patel SR, Crowley J, Reinke DK, Kuenkele KP, Chawla SP, et al. R1507, a monoclonal antibody to the insulin-like growth factor 1 receptor, in patients with recurrent or refractory Ewing sarcoma family of tumors: results of a phase II Sarcoma Alliance for Research through Collaboration study. *J Clin Oncol* 2011;29:4541–7.
- Du J, Bernasconi P, Claußer KR, Mani DR, Finn SP, Beroukhim R, et al. Bead-based profiling of tyrosine kinase phosphorylation identifies SRC as a potential target for glioblastoma therapy. *Nat Biotechnol* 2009;27:77–83.
- Grier HE, Krailo MD, Tarbell NJ, Link MP, Fryer CJ, Pritchard DJ, et al. Addition of ifosfamide and etoposide to standard chemotherapy for Ewing's sarcoma and primitive neuroectodermal tumor of bone. *N Engl J Med* 2003;348:694–701.
- Stahl M, Ranft A, Paulussen M, Bolling T, Vieth V, Bielack S, et al. Risk of recurrence and survival after relapse in patients with Ewing sarcoma. *Pediatr Blood Cancer* 2011;57:549–53.
- McDonald JW, Pilgram TK. Nuclear expression of p53, p21 and cyclin D1 is increased in bronchioalveolar carcinoma. *Histopathology* 1999;34:439–46.
- Schlaepfer DD, Hanks SK, Hunter T, van der Geer P. Integrin-mediated signal transduction linked to Ras pathway by GRB2 binding to focal adhesion kinase. *Nature* 1994;372:786–91.
- Roberts WG, Ung E, Whalen P, Cooper B, Hulford C, Autry C, et al. Antitumor activity and pharmacology of a selective focal adhesion kinase inhibitor, PF-562,271. *Cancer Res* 2008;68:1935–44.
- Mateo-Lozano S, Tirado OM, Notario V. Rapamycin induces the fusion-type independent downregulation of the EWS/FLI-1 proteins and inhibits Ewing's sarcoma cell proliferation. *Oncogene* 2003;22:9282–7.
- Mita MM, Mita AC, Chu QS, Rowinsky EK, Fetterly GJ, Goldston M, et al. Phase I trial of the novel mammalian target of rapamycin inhibitor deforolimus (AP23573; MK-8669) administered intravenously daily for 5 days every 2 weeks to patients with advanced malignancies. *J Clin Oncol* 2008;26:361–7.
- Zenali MJ, Zhang PL, Bendel AE, Brown RE. Morphoproteomic confirmation of constitutively activated mTOR, ERK, and NF-κappaB pathways in Ewing family of tumors. *Ann Clin Lab Sci* 2009;39:160–6.
- Clemente CF, Xavier-Neto J, Dalla Costa AP, Consonni SR, Antunes JE, Rocco SA, et al. Focal adhesion kinase governs cardiac concentric hypertrophic growth by activating the AKT and mTOR pathways. *J Mol Cell Cardiol* 2012;52:493–501.
- Thamilselvan V, Craig DH, Basson MD. FAK association with multiple signal proteins mediates pressure-induced colon cancer cell adhesion via a Src-dependent PI3K/Akt pathway. *FASEB J* 2007;21:1730–41.
- Cary LA, Han DC, Polte TR, Hanks SK, Guan JL. Identification of p130Cas as a mediator of focal adhesion kinase-promoted cell migration. *J Cell Biol* 1998;140:211–21.
- Nguyen DH, Webb DJ, Catling AD, Song Q, Dhakephalkar A, Weber MJ, et al. Urokinase-type plasminogen activator stimulates the Ras/Extracellular signal-regulated kinase (ERK) signaling pathway and MCF-7 cell migration by a mechanism that requires focal adhesion kinase, Src, and Shc. Rapid dissociation of GRB2/Sps-Shc complex is associated with the transient phosphorylation of ERK in urokinase-treated cells. *J Biol Chem* 2000;275:19382–8.
- Jawad MU, Cheung MC, Min ES, Schneiderbauer MM, Koniaris LG, Scully SP. Ewing sarcoma demonstrates racial disparities in incidence-related and sex-related differences in outcome: an analysis of 1631 cases from the SEER database, 1973–2005. *Cancer* 2009;115:3526–36.
- Granowetter L, Womer R, Devidas M, Krailo M, Wang C, Bernstein M, et al. Dose-intensified compared with standard chemotherapy for nonmetastatic Ewing sarcoma family of tumors: a Children's Oncology Group Study. *J Clin Oncol* 2009;27:2536–41.
- Ginsberg JP, Goodman P, Leisenring W, Ness KK, Meyers PA, Wolden SL, et al. Long-term survivors of childhood Ewing sarcoma: report from the childhood cancer survivor study. *J Natl Cancer Inst* 2010;102:1272–83.
- May WA, Lessnick SL, Braun BS, Klemsz M, Lewis BC, Lunsford LB, et al. The Ewing's sarcoma EWS/FLI-1 fusion gene encodes a more potent transcriptional activator and is a more powerful transforming gene than FLI-1. *Mol Cell Biol* 1993;13:7393–8.
- Gherardi E, Birchmeier W, Birchmeier C, Vande Woude G. Targeting MET in cancer: rationale and progress. *Nat Rev Cancer* 2012;12:89–103.
- Schaller MD, Borgman CA, Cobb BS, Vines RR, Reynolds AB, Parsons JT. pp125FAK a structurally distinctive protein-tyrosine kinase associated with focal adhesions. *Proc Natl Acad Sci U S A* 1992;89:5192–6.
- Mitra SK, Hanson DA, Schlaepfer DD. Focal adhesion kinase: in command and control of cell motility. *Nat Rev Mol Cell Biol* 2005;6:56–68.
- Schaller MD, Hildebrand JD, Shannon JD, Fox JW, Vines RR, Parsons JT. Autophosphorylation of the focal adhesion kinase, pp125FAK, directs SH2-dependent binding of pp60src. *Mol Cell Biol* 1994;14:1680–8.
- Zhang X, Chattopadhyay A, Ji QS, Owen JD, Ruest PJ, Carpenter G, et al. Focal adhesion kinase promotes phospholipase C-gamma1 activity. *Proc Natl Acad Sci U S A* 1999;96:9021–6.
- Han DC, Guan JL. Association of focal adhesion kinase with Grb7 and its role in cell migration. *J Biol Chem* 1999;274:24425–30.
- Chen HC, Appedu PA, Isoda H, Guan JL. Phosphorylation of tyrosine 397 in focal adhesion kinase is required for binding phosphatidylinositol 3-kinase. *J Biol Chem* 1996;271:26329–34.
- Aguirre Ghiso JA. Inhibition of FAK signaling activated by urokinase receptor induces dormancy in human carcinoma cells *in vivo*. *Oncogene* 2002;21:2513–24.

- 33.** Xu LH, Owens LV, Sturge GC, Yang X, Liu ET, Craven RJ, et al. Attenuation of the expression of the focal adhesion kinase induces apoptosis in tumor cells. *Cell Growth Differ* 1996;7:413–8.
- 34.** Hsia DA, Mitra SK, Hauck CR, Streblow DN, Nelson JA, Illic D, et al. Differential regulation of cell motility and invasion by FAK. *J Cell Biol* 2003;160:753–67.
- 35.** Jan YJ, Ko BS, Hsu C, Chang TC, Chen SC, Wang J, et al. Overexpressed focal adhesion kinase predicts a higher incidence of extrahepatic metastasis and worse survival in hepatocellular carcinoma. *Hum Pathol* 2009;40:1384–90.
- 36.** Ohali A, Avigad S, Zaizov R, Ophir R, Horn-Saban S, Cohen IJ, et al. Prediction of high risk Ewing's sarcoma by gene expression profiling. *Oncogene* 2004;23:8997–9006.
- 37.** Moritake H, Sugimoto T, Kuroda H, Hidaka F, Takahashi Y, Tsuneyoshi M, et al. Newly established Askin tumor cell line and overexpression of focal adhesion kinase in Ewing sarcoma family of tumors cell lines. *Cancer Genet Cytogenet* 2003;146:102–9.
- 38.** Pardali E, van der Schaft DW, Wiercinska E, Gorter A, Hogendoorn PC, Griffioen AW, et al. Critical role of endoglin in tumor cell plasticity of Ewing sarcoma and melanoma. *Oncogene* 2011;30:334–45.
- 39.** Bai Y, Li J, Fang B, Edwards A, Zhang G, Bui M, et al. Phosphoproteomics identifies driver tyrosine kinases in sarcoma cell lines and tumors. *Cancer Res* 2012;72:2501–11.
- 40.** Canel M, Secades P, Rodrigo JP, Cabanillas R, Herrero A, Suarez C, et al. Overexpression of focal adhesion kinase in head and neck squamous cell carcinoma is independent of fak gene copy number. *Clin Cancer Res* 2006;12:3272–9.
- 41.** Agochiya M, Brunton VG, Owens DW, Parkinson EK, Paraskeva C, Keith WN, et al. Increased dosage and amplification of the focal adhesion kinase gene in human cancer cells. *Oncogene* 1999;18:5646–53.
- 42.** Maurici D, Perez-Atayde A, Grier HE, Baldini N, Serra M, Fletcher JA. Frequency and implications of chromosome 8 and 12 gains in Ewing sarcoma. *Cancer Genet Cytogenet* 1998;100:106–10.
- 43.** Martins AS, Mackintosh C, Martin DH, Campos M, Hernandez T, Ordonez JL, et al. Insulin-like growth factor I receptor pathway inhibition by ADW742, alone or in combination with imatinib, doxorubicin, or vincristine, is a novel therapeutic approach in Ewing tumor. *Clin Cancer Res* 2006;12:3532–40.
- 44.** Emery CM, Vijayendran KG, Zipser MC, Sawyer AM, Niu L, Kim JJ, et al. MEK1 mutations confer resistance to MEK and B-RAF inhibition. *Proc Natl Acad Sci U S A* 2009;106:20411–6.
- 45.** Potratz JC, Saunders DN, Wai DH, Ng TL, McKinney SE, Carboni JM, et al. Synthetic lethality screens reveal RPS6 and MST1R as modifiers of insulin-like growth factor-1 receptor inhibitor activity in childhood sarcomas. *Cancer Res* 2010;70:8770–81.
- 46.** Naing A, LoRusso P, Fu S, Hong DS, Anderson P, Benjamin RS, et al. Insulin growth factor-receptor (IGF-1R) antibody cixutumumab combined with the mTOR inhibitor temsirolimus in patients with refractory Ewing's sarcoma family tumors. *Clin Cancer Res* 2012;18:2625–31.
- 47.** Hamamura K, Furukawa K, Hayashi T, Hattori T, Nakano J, Nakashima H, et al. Ganglioside GD3 promotes cell growth and invasion through p130Cas and paxillin in malignant melanoma cells. *Proc Natl Acad Sci U S A* 2005;102:11041–6.
- 48.** Tamura M, Gu J, Takino T, Yamada KM. Tumor suppressor PTEN inhibition of cell invasion, migration, and growth: differential involvement of focal adhesion kinase and p130Cas. *Cancer Res* 1999;59:442–9.
- 49.** Infante JR, Camidge DR, Mileskkin LR, Chen EX, Hicks RJ, Rischin D, et al. Safety, pharmacokinetic, and pharmacodynamic phase I dose-escalation trial of PF-00562271, an inhibitor of focal adhesion kinase, in advanced solid tumors. *J Clin Oncol* 2012;30:1527–33.

Cancer Research

The Journal of Cancer Research (1916–1930) | The American Journal of Cancer (1931–1940)

High-Throughput Tyrosine Kinase Activity Profiling Identifies FAK as a Candidate Therapeutic Target in Ewing Sarcoma

Brian D. Crompton, Anne L. Carlton, Aaron R. Thorner, et al.

Cancer Res 2013;73:2873-2883. Published OnlineFirst March 27, 2013.

Updated version Access the most recent version of this article at:
doi:[10.1158/0008-5472.CAN-12-1944](https://doi.org/10.1158/0008-5472.CAN-12-1944)

Supplementary Material Access the most recent supplemental material at:
<http://cancerres.aacrjournals.org/content/suppl/2013/03/22/0008-5472.CAN-12-1944.DC1>

Cited articles This article cites 49 articles, 28 of which you can access for free at:
<http://cancerres.aacrjournals.org/content/73/9/2873.full.html#ref-list-1>

Citing articles This article has been cited by 3 HighWire-hosted articles. Access the articles at:
[/content/73/9/2873.full.html#related-urls](http://cancerres.aacrjournals.org/content/73/9/2873.full.html#related-urls)

E-mail alerts [Sign up to receive free email-alerts related to this article or journal.](#)

Reprints and Subscriptions To order reprints of this article or to subscribe to the journal, contact the AACR Publications Department at
pubs@aacr.org.

Permissions To request permission to re-use all or part of this article, contact the AACR Publications Department at
permissions@aacr.org.